Geophysical Research Letters

RESEARCH LETTER
10.1029/2023GL107667

Investigating the Interaction Between Transboundary Haze and Planetary Boundary Layer in Singapore

T. Huang[1,2], T. Fang[2], L. Feng[2,3], C. Y. Leong[2], and S. H. L. Yim[1,2,3]

[1]Lee Kong Chian School of Medicine, Nanyang Technological University, Singapore, Singapore, [2]Earth Observatory of Singapore, Nanyang Technological University, Singapore, Singapore, [3]Asian School of the Environment, Nanyang Technological University, Singapore, Singapore

T. Huang and T. Fang contributed equally to this work.

Key Points:

- Nocturnal low-level jet created favorable conditions for haze transport to Singapore when hotspot numbers increased in Indonesia
- Diurnal increase in planetary boundary layer height facilitated the mixing of transboundary haze and ground-level aerosols
- Source apportionment shows that fire and other sectoral emissions in Indonesia influenced the southern part of Peninsular Malaysia

Supporting Information:

Supporting Information may be found in the online version of this article.

Correspondence to:

S. H. L. Yim,
yimsteve@gmail.com

Citation:

Huang, T., Fang, T., Feng, L., Leong, C. Y., & Yim, S. H. L. (2024). Investigating the interaction between transboundary haze and planetary boundary layer in Singapore. *Geophysical Research Letters*, *51*, e2023GL107667. https://doi.org/10.1029/2023GL107667

Received 9 DEC 2023
Accepted 14 FEB 2024

Author Contributions:

Conceptualization: S. H. L. Yim
Data curation: T. Huang, T. Fang
Formal analysis: T. Huang, T. Fang, S. H. L. Yim
Funding acquisition: S. H. L. Yim
Investigation: T. Huang, T. Fang, S. H. L. Yim
Methodology: T. Huang, T. Fang, L. Feng, C. Y. Leong
Resources: S. H. L. Yim
Software: T. Huang, T. Fang
Supervision: S. H. L. Yim

Abstract Transboundary air pollution is one of the critical environmental problems in Southeast Asia; nevertheless the interaction between transboundary haze and local planetary boundary layer (PBL) remains unclear due to a lack of sufficient observations and sophisticated simulations. This study applied LiDAR observations and model simulations to comprehensively evaluate the interaction between transboundary haze and local PBL during a recent transboundary haze episode in Singapore in October 2023. Results show that upper-level southeasterly wind, especially the nocturnal low-level jet, created favorable conditions for aerosol transport when fire hotspot numbers increased in Indonesia. The rapid diurnal increase in PBL height facilitated the entrainment of upper-level haze into the PBL, interacting with ground-level aerosols through turbulent mixing. Model simulations further show the significant contributions of fire emissions to the transboundary haze episode in maritime Southeast Asia. The impacts extended toward the southern region of Peninsular Malaysia, driven by the persistent prevailing southeasterly wind.

Plain Language Summary In Southeast Asia, transboundary air pollution that crosses borders is a significant environmental issue. However, we don't fully understand how the remote haze interacts with local upper-level atmosphere. Our study used LiDAR observations and model simulations to thoroughly examine this problem during a recent episode in Singapore in October 2023. Our findings indicate that upper-level southeasterly wind, particularly a low-level jet during the night, played a crucial role in transporting aerosols when there was an increase in fire hotspot numbers in Indonesia. In the daytime, the rise of planetary boundary layer (PBL) height helped drive the upper-level haze into the PBL, where it mixed with aerosols near the ground through the vertical movement of air parcels. Additionally, our simulations revealed that emissions from fires significantly contributed to the transboundary haze episode in maritime Southeast Asia. The impact of this haze extended toward the southern region of Peninsular Malaysia, primarily due to the persistent southeasterly wind prevailing in the area.

1. Introduction

In addition to localized air pollution, transboundary air pollution has emerged as a crucial factor exacerbating air pollution on global (Holloway et al., 2003), regional (Gu & Yim, 2016; Hou et al., 2019), and local scales (Tong et al., 2018; Huang, Li, et al., 2021). Particularly, transboundary haze stemming from biomass burning has been a prominent issue throughout Southeast Asia (Hansen et al., 2019). Comprehensive instrumentation, including the Aerosol Robotic Network (AERONET, Holben et al., 1998) and a micro-pulse LiDAR Network (MPLNET, Welton et al., 2001) within the framework of the Seven Southeast Asian (7-SEAS, Reid et al., 2013) initiative (Chew et al., 2013), has been implemented to monitor the transboundary haze in this region. In the context of climate change, there is an increasing need for proactive measures to shield people in this region from the adverse effects of transboundary haze.

Transboundary haze influences local ground-level air quality by its interaction with the planetary boundary layer (PBL), especially through vertical movement of air parcels (Hogan et al., 2009; Slater et al., 2020). To explore this mechanism, prior studies have applied large-eddy simulations (LES) and found that a positive feedback loop exists between aerosols and PBL height in urban $PM_{2.5}$ episodes (Slater et al., 2021, 2022). Specifically, increased aerosol concentration reduces the buoyant turbulence, leading to a drop in the PBL height. This further limits the vertical mixing of aerosol in the atmosphere volume, resulting in an increased aerosol loading. Nevertheless, the ingress of transboundary aerosols into the PBL was not considered, which is a pivotal step in deteriorating

Validation: T. Huang, T. Fang
Visualization: T. Huang
Writing – original draft: T. Huang, T. Fang
Writing – review & editing: L. Feng, C. Y. Leong, S. H. L. Yim

ground-level air quality via turbulent mixing (Geiß et al., 2017; Tang et al., 2016; Zhu et al., 2018). Furthermore, the mechanism during nighttime is complicated because nocturnal low-level jet (LLJ) also plays a vital role in urban haze formation (Tsiringakis et al., 2022). More evidence is needed from direct observations of haze in the upper atmosphere to understand the interaction mechanism between transboundary haze and PBL.

Chemical transport modeling and source apportionment techniques, revealing the haze dynamics and source contributions of species and sectors to transboundary haze, are of importance to understand the haze formations and their impacts on air quality (Lelieveld et al., 2015). Prior study indicated that biomass burning aerosols constituted a substantial portion, approximately 40%–60%, of haze events in major Southeast Asian cities during 2003–2004 (Lee et al., 2017). Previous study reported fire emissions contributed the most to $PM_{2.5}$ in maritime Southeast Asia during haze events (~23.0%–68.6%), meanwhile, other sectoral contributors such as industrial process and transportation also accounted for a certain part of the haze formations (Fang et al., 2023). For Singapore, recent research suggested that haze events are primarily attributable to biomass burning emissions from Indonesia during the haze seasons from August to October, whereas Peninsular Malaysia becomes a larger source to Singapore during off-season haze events (Hansen et al., 2019). Existing research has explored the general transboundary haze characteristics during an event, but the detailed temporal and vertical variations are also necessary to comprehend the haze formation and its interactions with various atmospheric processes such as the PBL height development. It is still of great importance to extend the existing modeling studies to a more detailed level by incorporating temporal and vertical process analyses.

Synergistic observations of wind and aerosol vertical profiles in the upper-level atmosphere are critical for comprehensively understanding the mechanism of transboundary haze in Southeast Asia. Doppler LiDAR, which is an active optical remote sensing equipment, can retrieve wind and aerosol vertical profiles simultaneously at high temporal and range resolutions (Barlow et al., 2011; Manninen et al., 2018; Pearson et al., 2009; Tonttila et al., 2011, 2015). The effectiveness of Doppler LiDAR has been demonstrated in numerous studies focusing on the mixing layer and turbulence (O'Connor et al., 2005, 2010; Yim, 2020). While LiDAR network provides detailed vertical profiles of upper atmosphere, it faces limitations in achieving high spatial coverage of extensive regions such as Southeast Asia. Numerical modeling can address this limitation by providing spatial information. With the recent deployment of a Doppler LiDAR unit in Singapore, we are now equipped to verify model outputs using upper-level observations of aerosol and wind, thus enhancing our understanding of the mechanisms underlying transboundary haze.

This study employed LiDAR observations and the Comprehensive Air Quality Model with Extensions (CAMx) simulations to investigate the processes and sources of a recent transboundary haze episode that occurred during 6th–7th October, 2023. Detailed information regarding LiDAR and model configurations is provided in Section 2, while the results of transboundary haze monitoring, aerosol-PBL interactions, and source attribution are presented in Section 3.

2. Data and Methods

2.1. LiDAR Observation of Upper-Level Atmosphere

To measure the profile of aerosol and wind information in the upper-level atmosphere in Singapore, we installed one unit of Halo Photonics StreamLine XR Doppler LiDAR (DL226) on the rooftop of N2 Building (1.35 N, 103.68 E) on the campus of Nanyang Technological University, Singapore (Figure S1 in Supporting Information S1). Detailed specifications are listed in Table S1 in Supporting Information S1. The LiDAR can detect up to 12 km above ground level with a range resolution of 60 m, and is operating in two modes: Stare and Velocity Azimuth Display (VAD). In Stare mode, LiDAR emitted laser pulses every second to derive the vertical velocity and signal-to-noise ratio (SNR). The performance of Halo Doppler LiDAR in wind measurement has been thoroughly tested and confirmed during the past 5 years of application of the same LiDAR model in Hong Kong (Yim, 2020). Attenuated backscatter coefficient (β) profile was retrieved based on the SNR profile when telescope focus length function of the LiDAR unit is known (Pentikäinen et al., 2020; Huang, Yang, et al., 2021). The focus length in DL226 was set to infinite by the manufacturer. PBL height was derived by the hourly average of heights where absolute maximum gradient of β occurs. Cloud or hydrometeor was detected when $\beta > 3.5 \times 10^{-5}$. In VAD mode, LiDAR scanned with 6 beams rotating every 60° in azimuth at an elevation angle of 75° every 10 min to derive horizontal wind speed and direction. Based on horizontal wind profiles, algorithm presented by Tuononen et al. (2017) and Manninen et al. (2018) was applied to derive LLJ.

2.2. Numerical Model Simulations

To simulate $PM_{2.5}$ concentration and the source contribution, this study employed the CAMx in version 7.2 driven by the meteorology conditions from the Weather Research & Forecasting Model (WRF) in version 4.0 (Dunker et al., 2019; Karamchandani et al., 2017; Li et al., 2022). Anthropogenic emission data was re-gridded from the Copernicus Atmosphere Monitoring Service (CAMS) global Emission Inventories (EIs) at a spatial resolution of $0.1° \times 0.1°$ (Granier et al., 2019). Biogenic emissions were also derived from the CAMS global EIs at a spatial resolution of $0.25° \times 0.25°$ calculated using the MEGAN model version 2.1 (Guenther et al., 2012). Daily open fire emissions were obtained from satellite observations by the Fire Inventory from the National Center for Atmospheric Research (FINN) dataset (Wiedinmyer et al., 2011). A two-nested modeling domain at a spatial resolution of 30 and 10 km was set for $PM_{2.5}$ simulations (Figure S1 in Supporting Information S1). The first domain (D1) covered the entire Southeast Asia, while the second domain (D2) included Singapore and most of the maritime Southeast Asia. Vertical processes contained nine layers from the surface to the top level at 50 hPa. The Carbon Bond version 6 (CB6) and coarse and fine (CF) mechanisms were selected for gas-phase (Yarwood et al., 2010) and aerosol (Gaydos et al., 2007; Meroni et al., 2017) chemistry simulations, respectively. Initial and boundary conditions for D1 utilized the default profiles, and those for D2 were retrieved from the simulation results in D1. Although the episode occurred during 6th–7th October, the simulation period of CAMx considered two additional days before and after the episodes as a reference. Also, two additional spin-up days were pre-simulated to exclude the impacts of initial conditions.

Two scenarios were chosen for model simulations in D2. One was the baseline scenario exhibiting the spatial and temporal $PM_{2.5}$ variations during the episode. Process analysis was also activated in the baseline scenario to characterize the time series contributions of different physical and chemical processes to $PM_{2.5}$ formations (Liu et al., 2010; Ma et al., 2021). Another one was the control scenario without fire emissions. Fire contributions to the episode can be subsequently represented by the differences between the $PM_{2.5}$ concentration under baseline and control scenarios.

Model evaluation results in Figure S2 in Supporting Information S1 indicate good agreement between observed and simulated meteorology conditions during the simulation period. The correlation coefficient (R) between the simulated and LiDAR-detected PBL height was 0.83, with a Normalized Mean Bias (NMB) of −17.80%. The R value for temperature and relative humidity (RH) reached 0.92 and 0.90, respectively. Wind simulation has been challenging in various models because of its high uncertainty and variability (Yu et al., 2022). Hence the R for wind speed (WS) was relatively lower (0.53). The NMB values for temperature, RH, and WS were −12.22%, 10.65%, and −24.27%, respectively. These results were comparable with those reported in other research (Tong et al., 2018; Wei et al., 2018; Yang et al., 2022). The R and NMB for $PM_{2.5}$ simulations were 0.74 and 22.16%, respectively, attaining the criteria (NMB $< \pm 30\%$ and $R > 0.4$) recommended by Emery et al. (2017).

2.3. Surface Level Observations of Meteorology, $PM_{2.5}$ Concentration, and Hotspots

Hourly measurements of $PM_{2.5}$ concentration at 5 sub-regions of Singapore were obtained from the website of National Environmental Agency (NEA, https://www.haze.gov.sg/, last accessed on 10th October 2023). Hourly ground-level meteorological records were collected from the website of Meteorological Service Singapore (MSS, https://www.weather.gov.sg/home/, last accessed on 10th October 2023). Hotspot data in Southeast Asia was extracted from the Moderate Resolution Imaging Spectroradiometer (MODIS) detections from NASA's Fire Information for Resource Management System (FIRMS) (https://earthdata.nasa.gov/firms, last accessed on 10th October 2023).

3. Results

3.1. Ground- and Upper-Level Observations During the Transboundary Haze Episode

Figure 1a illustrates a significant upward trend (1.3 $\mu g/m^3$/hr, $R^2 = 0.93$) in the national-mean surface concentration of $PM_{2.5}$, starting at 03:00 on October 6th, in Singapore. The peak concentration reached 65.6 $\mu g/m^3$ at 17:00 on October 7th, marking a substantial 500% increase compared to the lowest level (11 $\mu g/m^3$) recorded at 03:00 on October 6th. Subsequently, $PM_{2.5}$ concentration exhibited a rapid decline, falling to 26 $\mu g/m^3$ by 02:00 on October 8th, and remained relatively low during the daytime hours (07:00–12:00) of October 8th, with a

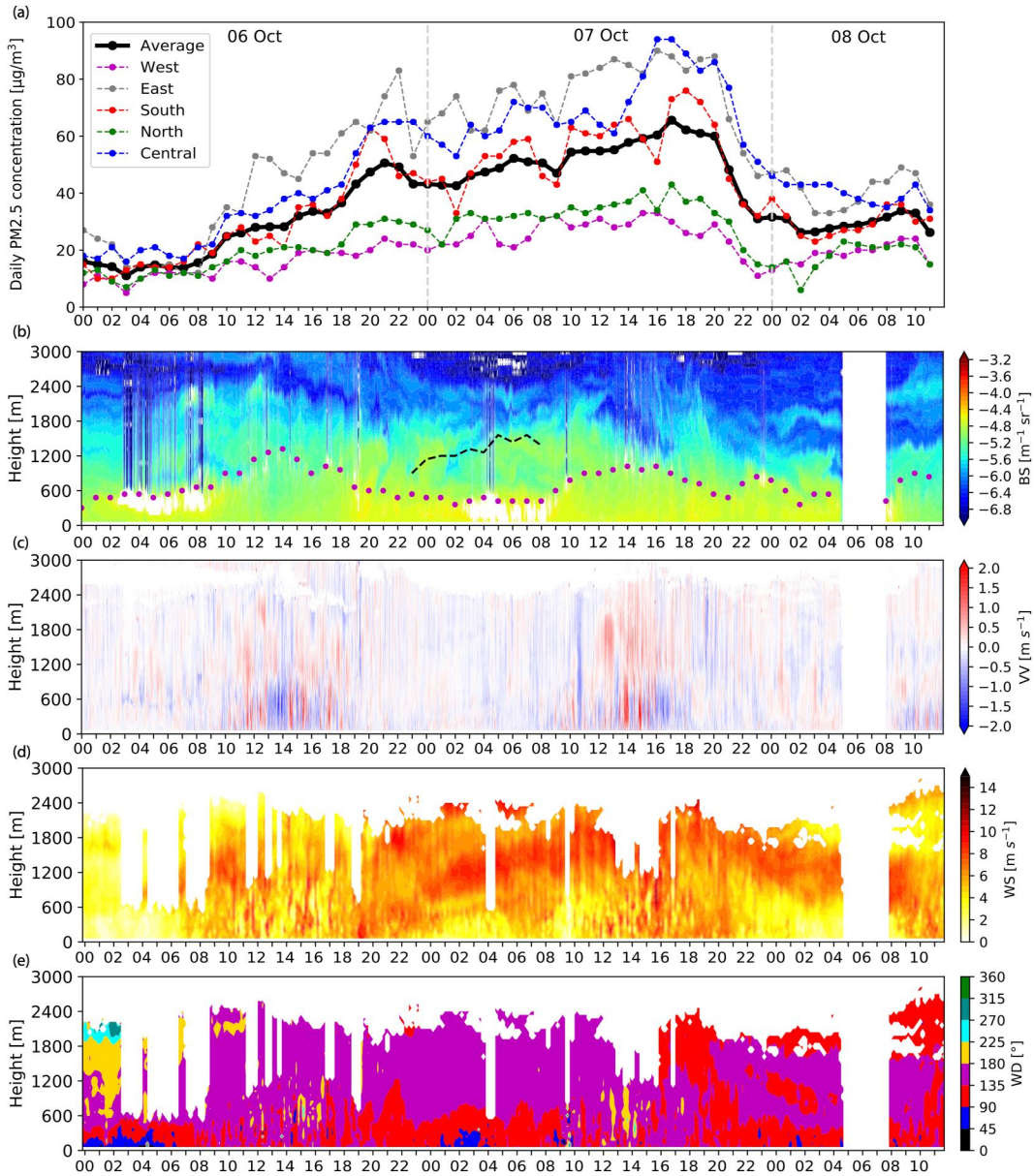

Figure 1. Ground- and upper-level measurements from 00:00 (LST) on October 6th to 12:00 (LST) on 8th October 2023, in Singapore. (a) Ground-level measurements of hourly $PM_{2.5}$ concentration at West, East, South, North, and Central Singapore. (b) Height-time profile of aerosol attenuated backscatter coefficient during the episode. Clouds (white) are removed. Magenta dots represent hourly PBL height. Black dash line indicates the position of nocturnal LLJ. (c) Height-time profile of vertical velocity. Positive values represent updrafts. (d) Height-time profile of horizontal wind speed and (e) Height-time profile of horizontal wind direction.

temporal mean value of 31 μg/m^3. Notably, among the five sub-regions in Singapore, the Central and East regions exhibited higher pollutant concentration in comparison to the other areas.

On October 6th, the highest PBL height was observed at 14:00, reaching 1,560 m above ground, accompanied by substantial turbulent mixing (Figures 1b and 1c). Figure 1b depicts that PBL height experienced a rapid descent to 660 m after sunset (at 19:00), attributed to the diminished surface heating, leaving residual layers above the boundary layer. Figure 1b shows a nocturnal LLJ emerged at or above 1,200 m above ground at 23:00, coinciding with substantial aerosol loading observed at the same altitude. Figure 1d reveals the magnitude of the jet nose, averaged from 23:00 on October 6th to 7:00 on October 7th, was measured approximately at 10 m/s. Furthermore,

Figure 1e highlights the southeast origin of the LLJ, representing favorable conditions for the transport of fire smoke emissions from 771 hotspots in Indonesia (Figure S3 in Supporting Information S1) to Singapore.

Transboundary haze can interact with local PBL development, contributing to the deterioration of air quality within the boundary layer. On normal days with local emissions only, the development of diurnal PBL improves the surface air quality by turbulent mixing, while it deteriorates the surface air quality during transboundary air pollution episodes (Huang, Li, et al., 2021). In Figure 1b, transboundary haze hardly mixed with local aerosol within the PBL during the nighttime period from 23:00 on October 6th to 7:00 on October 7th due to atmospheric stratification. After sunrise at 7:00 on October 7th, a rapid PBL development occurred, driven by the recovery of surface heating and turbulent mixing. By 12:00 on October 7th, a complete contact of two aerosol layers took place when PBL height reached above 1,000 m. Boundary layer top entrainment, as indicated by cloud top features (depicted as white patches in Figure 1b), in conjunction with vigorous turbulent mixing (Figure 1c) induced by surface heating, effectively mixed the aerosols within PBL. This resulted in a peak in surface concentration observed at 17:00 on October 7th in Figure 1a. Subsequently, the removal of air pollution from the PBL occurred after 17:00 driven by the relatively stronger upper atmospheric advection and a reduction in fire hotspot numbers in Indonesia (specifically, a 67% decrease compared to those on October 6th). No transboundary haze was observed during both daytime and nighttime on October 8th. The observational results from ground- and upper-level measurements illustrate the comprehensive transport and interaction processes of the recent transboundary haze episode.

3.2. Model Simulation and Source Apportionment of the Haze Episode in Singapore

Figure 2a depicts the diurnal variation of vertical $PM_{2.5}$ concentration and PBL in Singapore. The development of PBL, particularly the daytime peak PBL height during 6th and 7th October, was accurately simulated by our model and consistent with the LiDAR results (Figure S2 in Supporting Information S1). Our model successfully captured the presence of transboundary haze above the PBL height from 9:00 to 15:00 on October 6th–7th, consistent with the LiDAR observations when two aerosol layers contacted. This transboundary contribution above the PBL height to surface $PM_{2.5}$ concentration reached 5.8 $\mu g/m^3$ as presented in Figure 2b. During the same period On October 5th, 6th, and 8th, the contribution above the PBL height was only 2.3 $\mu g/m^3$, 2.8 $\mu g/m^3$, and 1.1 $\mu g/m^3$, respectively. The result clearly shows that the nocturnal LLJ from 23:00 on October 6th to 7:00 on October 7th facilitated the transboundary haze aloft to Singapore. Then the surface $PM_{2.5}$ levels increased when two aerosol layers mixed due to the PBL development during the daytime on October 7th. The persistence of transboundary haze aloft during the nocturnal period (23:00–5:00) was also reproduced by the model as shown in Figure 1a. Additionally, the simulated surface peak value (71.6 $\mu g/m^3$) at 19:00 on October 7th was comparable to the observed peak ground-level pollutant concentration (65.6 $\mu g/m^3$).

Figure 2b indicates the contributions of individual atmospheric processes to the average $PM_{2.5}$ concentration from the ground to about 1.7 km. The positive and negative contributions mean the $PM_{2.5}$ generation and removal, respectively, caused by the individual processes. Notably, the south boundary process (i.e., the total contributions of horizontal and vertical advection and diffusion processes from outside of the south boundary defined in Figure S1 in Supporting Information S1) to Singapore appeared on October 5th and became the major cause of vertical $PM_{2.5}$ accumulations during the daytime on October 6th and 7th. The result proves transboundary pollution from Indonesia could be the main reason inducing this haze episode in Singapore. The organic and inorganic aerosol chemistry contributions were also apparent for secondary $PM_{2.5}$ formations during the daytime. This is because the stronger solar radiation in the daytime promoted the oxidation reaction of gasoline pollutants to form organic or inorganic aerosols. The role of south boundary process in surface $PM_{2.5}$ accumulations was also crucial on October 6th and 7th. After this, a notable decrease in the contributions from the south boundary process was found for both the surface and vertical average $PM_{2.5}$ on October 8th, which was consistent with the decline in ground-level $PM_{2.5}$ observations (Figure 1a). Besides, we noted the consecutively obvious contributions from local area emissions to surface $PM_{2.5}$ formations during the whole simulation period. These contributions could be mainly from the local ground-level sectoral emissions such as transportation and industry.

Moreover, the model reported that fire contributions were 8.3 $\mu g/m^3$ on October 5th, which then escalated on October 6th (10.0 $\mu g/m^3$) and 7th (15.5 $\mu g/m^3$) to accelerate the haze episode in Singapore (Figure 2d). This could be highly related to the intensified fire activities in Indonesia, consistent with the observed increase in hotspots during this period (Figure S3 in Supporting Information S1). The subsequent drop-down of fire contributions on

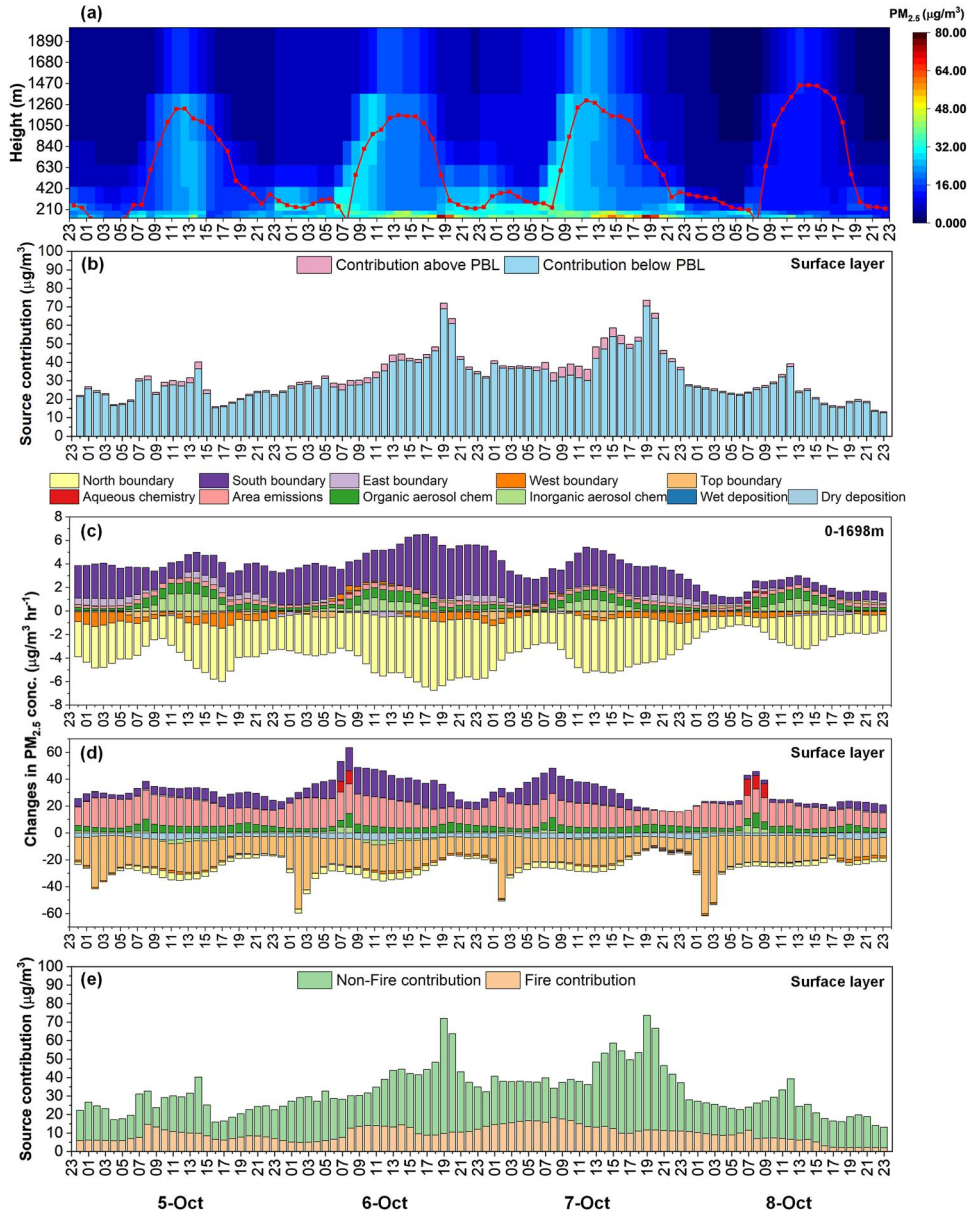

Figure 2. Model simulation results from 00:00 (LST) on October 5th to 23:00 (LST) on October 8th 2023, including the transboundary episode (October 6th–7th) in Singapore. (a) Diurnal variation in the vertical $PM_{2.5}$ concentration averaged within Singapore. The red line refers to the PBL height simulated by the model. (b) Emission contributions above and below PBL height to surface $PM_{2.5}$ concentration in Singapore during the episode. Individual atmospheric process contributions to (c) Column-averaged $PM_{2.5}$ concentration from surface to ~1.7 km above ground and (d) surface $PM_{2.5}$ concentration in Singapore. (e) Source apportionment of non-fire and fire contributions to surface $PM_{2.5}$ concentration in Singapore during the episode. Note that the north, south, east, west, and top boundaries in (c) and (d) mean the contributions of horizontal and vertical advection and diffusion processes from different directions out of the boundaries defined in Figure S1 in Supporting Information S1 to Singapore.

October 8th (5.7 μg/m^3) aligned with the observational findings (Figure 1) and the dramatic decrease in the hotspots number (Figure S3 in Supporting Information S1). Non-fire emission contributions to $PM_{2.5}$ concentration also elevated on October 6th and 7th, particularly at the modeled peak time (19:00–20:00). This is probably because some near-surface source contributions such as transportation were hardly to disperse with the decline in PBL height since 19:00, resulting in an accumulation of $PM_{2.5}$ concentration.

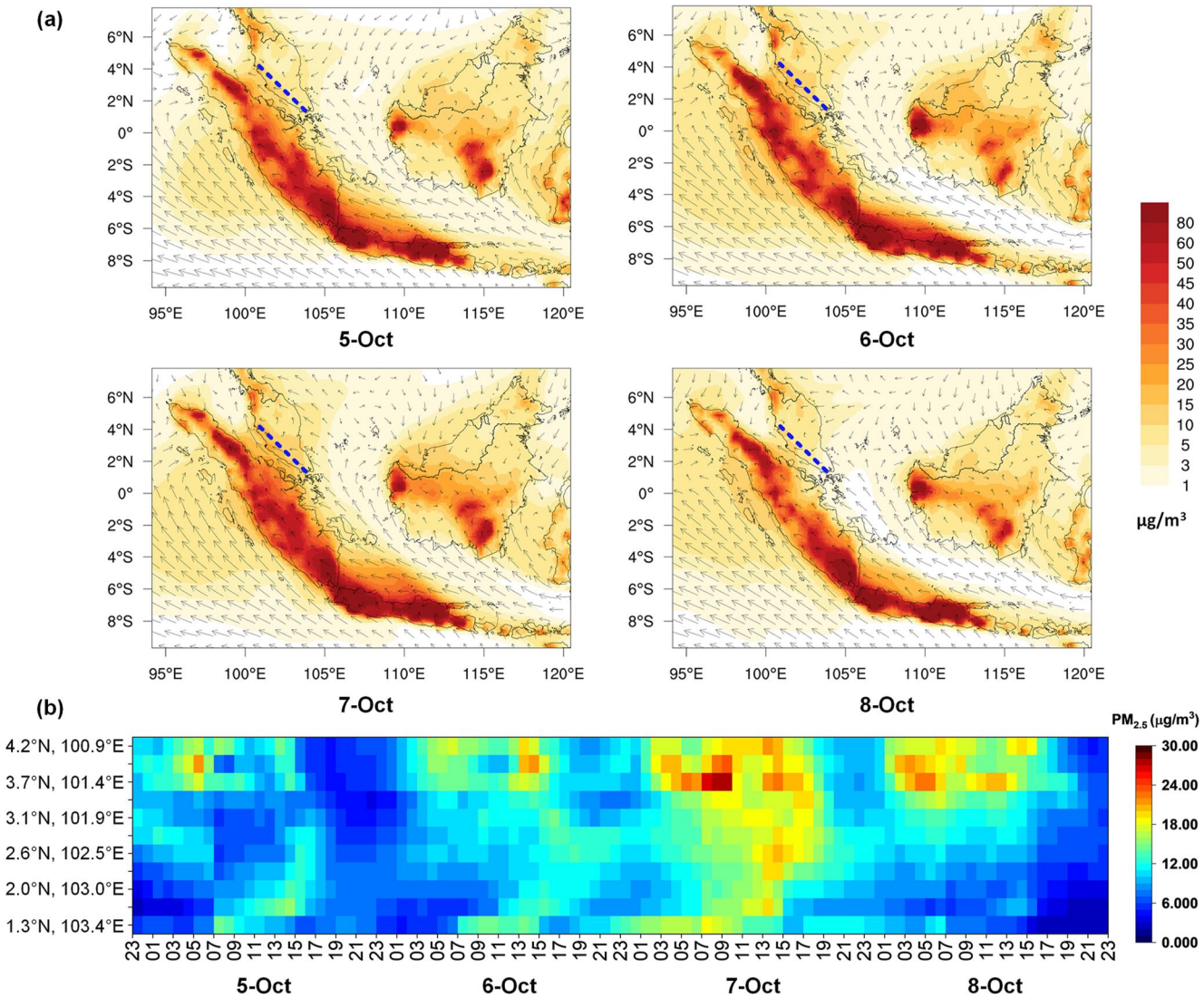

Figure 3. (a) Spatial distribution of fire contribution to surface $PM_{2.5}$ concentration in maritime Southeast Asia with wind directions (black arrow). (b) The time series of fire contribution to surface $PM_{2.5}$ concentration along the geographical locations from Singapore to the southern part of Peninsular Malaysia as shown along the blue dashed lines in (a).

3.3. Spatiotemporal Characteristics of the Transboundary Haze Episode in Maritime Southeast Asia

According to the spatial results, the fire contributions to $PM_{2.5}$ concentration in Singapore and southern parts of Peninsular Malaysia were observed on October 5th. Then, the fire contributions became more extensive and elevated on October 6th and 7th but shrinked on October 8th (Figure 3a). In Indonesia, the spatial fire contributions kept at a high and intensive level on all days because of its local persistent burning activities (Figure S3 in Supporting Information S1).

Driven by dominant southeasterly wind during the episode (Figure 3a), transboundary haze extended to the southern parts of Peninsular Malaysia. Figure 3b illustrates the variation in fire contributions to surface $PM_{2.5}$ concentration across the geographical locations along the direction from Singapore to the southern part of Peninsular Malaysia. The results demonstrated a clear northwesterly movement of fire pollution particularly from 11:00 to 19:00 on October 7th, spanning from 1.3°N to 4.2°N and 100.9°E to 103.4°E with the coverage of Kuala Lumpur (i.e., 3.1°N, 101.6°E). Accordingly, transboundary pollution could affect not only Singapore but also Peninsular Malaysia. Besides, we found fire contribution levels in the relative northern locations (i.e., 3.7°N−4.2°N and 100.9°E−101.4°E) were already notably high from 3:00 to 10:00 on October 7th before the transboundary

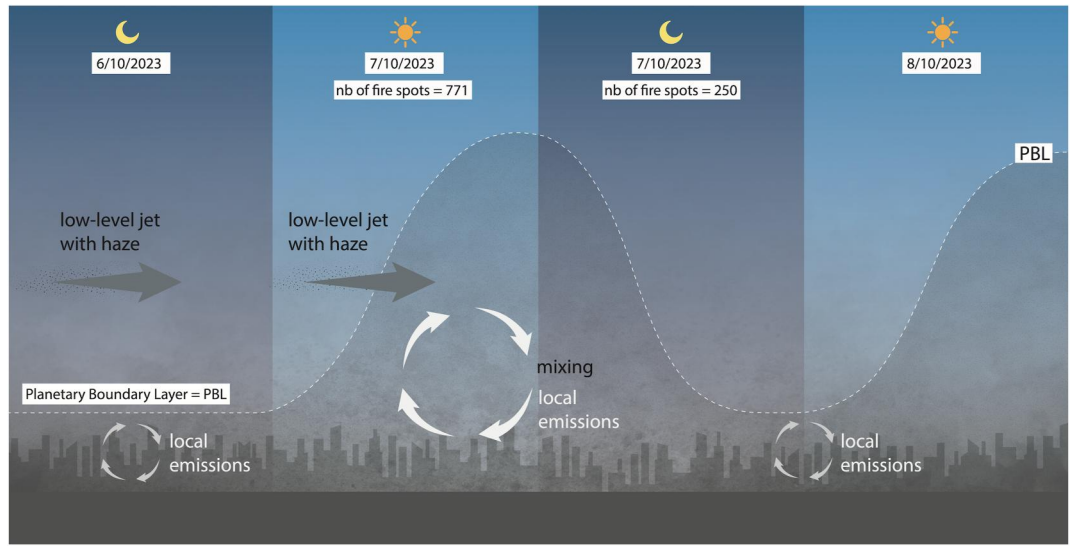

Figure 4. Diagram of the interaction between the transboundary haze and the PBL development during the episode. During the nighttime of October 6th, a nocturnal LLJ from the southeast transported haze originating from the fire hotspots in Indonesia to Singapore. Due to the stabilization of atmosphere in the nighttime, transboundary haze cannot sufficiently mix with local aerosol within PBL. Subsequently, with the rapid increase in PBL height following sunrise on October 7th, transboundary haze was entrained into the top of the PBL, participating in interaction with ground-level aerosols through vigorous turbulent mixing in the daytime. The surface concentration reached the peak value at 17:00 on October 7th. Governed by surrounding fire hotspots and the north-westward movement of transboundary haze, surface concentration experienced a rapid decline in Singapore after the peak time. On October 8th, no transboundary haze was observed, neither during the daytime nor at nighttime.

haze happened. This could be associated with the occurrence of some scattered local fire activities in Malaysia (Figure S3 in Supporting Information S1). When transboundary pollution happened from 11:00 to 19:00, fire contributions to these locations were not comparable to those from 3:00 to 10:00 but still significant. This suggests that both local and transboundary pollution due to the fire activities were of importance for the haze event in Malaysia.

4. Discussion and Conclusions

This study illustrated the mechanisms underlying the interaction between transboundary haze and PBL development during a recent transboundary haze episode in Singapore in October 2023 (Figure 4) using Doppler LiDAR observations alongside model simulations. Overall, the interaction of local PBL development and transboundary haze played a critical role in the formation of the episode during October 6th and 7th, 2023. The Doppler LiDAR observations provided an evident association between the transboundary haze episode and southeasterly wind in Singapore. The occurrence of a nocturnal LLJ created favorable conditions for the transport of biomass burning haze when fire hotspot numbers in Indonesia inclined. After that, increased PBL height facilitated the entrainment of transboundary haze into the PBL top and then the interaction with ground-level aerosols through vigorous turbulent mixing in the daytime. Model simulations of the haze episode exhibited consistency with both ground-level observations and LiDAR results. The contributions from fires in the south boundary of the model accounted for the haze formations in Singapore. This haze episode manifested distinct transboundary characteristics over the maritime Southeast Asian region, evident in both spatial and temporal scales. Moreover, the contributions of fires can extend from Singapore to the southern part of Peninsular Malaysia, primarily driven by the prevailing southeasterly wind.

Long-range transport of biomass aerosols by LLJs is a crucial mechanism in the formation of haze episodes. Utilizing reanalysis data and AERONET observations, Huang et al. (2020) identified the significant role of a westerly LLJ at 700 hPa (around 3 km above ground) in facilitating the transport of biomass burning aerosols from Indochina to the West Pacific region. Although the nocturnal LLJ in our study was lower (1,200 m) in altitude compared to 700 hPa, it remained sufficiently elevated to transport haze from Indonesia to Singapore and

even to Peninsular Malaysia. Cheng et al. (2022) used a combination of field campaigns and model simulations to demonstrate that PBL enhances turbulent mixing during daytime, thereby regulating the vertical distribution of transported air pollution induced by sea-breeze in Taiwan. This mechanism aligns with our findings, indicating that local PBL development intensifies the vertical mixing of transboundary haze with local aerosols, consequently exacerbating surface air quality. Some studies outside Southeast Asia also reported the role of nocturnal LLJ in transboundary air pollution. For example, Sullivan et al. (2017) used LiDAR observations to reveal that the onset of nocturnal LLJ transported polluted O_3 to Mid-Atlantic US and enhanced the downward transport of pollutant to the surface level, influencing the "next-day" air quality. It confirms the mechanism revealed in this study conducted in Southeast Asia. A recent global nocturnal LLJ review study demonstrated a certain level of LLJ frequency in Southeast Asia (Algarra et al., 2019), indicating the significance of understanding the role of LLJ (Text S1 and Figure S4 in Supporting Information S1) and interaction of air pollutants below and above the PBL. Furthermore, Singapore reveals a more pronounced diurnal PBL height variation compared to Hong Kong, which is a subtropical coastal area influenced by transboundary haze from inland China, indicating its robust mixing capacity in the tropics (Huang, Li, et al., 2021). As a part of the 7SEAS program (Reid et al., 2013), AERONET and MPLNET have served as crucial tools to provide remote sensing measurements of aerosol vertical distribution in Southeast Asia. These measurements play a pivotal role in monitoring and investigating transboundary haze in the region. With critical vertical upper-level wind information provided by our LiDAR unit, the understanding of transboundary haze will be improved in the future.

Reducing uncertainty in source apportionment is vital. Hyer and Chew (2010) used model simulations to indicate that biomass burning smoke contributed to nearly all the peak PM_{10} events during September–November 2006, but the specific contribution of smoke was unknown due to the large uncertainty in models. Uncertainty in these results mostly originated from the emissions and the meteorology (Hertwig et al., 2015). To address this, Atwood et al. (2013) suggested that the role of upper-level vertical wind shear and mixing down through the boundary layer may need to be considered in the future source apportionment. In our study, model results were first compared with upper-level LiDAR observations, particularly with PBL characteristics to reduce the uncertainty, and eventually revealed the largest contribution from south boundary of the model to the haze event, which was consistent with the results for PM_{10} simulations in Hansen et al. (2019). Overall, with a numerical model validated by LiDAR observation, we can better understand the sources of the haze episode in Singapore.

While the findings of this study contribute to the understanding of the underlying mechanisms of transboundary haze and source apportionment in Southeast Asia, it is still critical to work firmly with existing instrumentation deployed in Southeast Asia such as those under the 7SEAS project. Our forthcoming established Doppler LiDAR network in Singapore is expected to advance the capabilities in observing upper-level aerosol and wind profiles in this region. These advancements can significantly enhance our ability to forecast air pollution in Southeast Asia.

Data Availability Statement

Surface $PM_{2.5}$ and meteorological data can be found at https://www.haze.gov.sg/ and http://www.weather.gov.sg/mobile/current-temperature/. Hotspot data in Southeast Asia was extracted from the Moderate Resolution Imaging Spectroradiometer (MODIS) detections from NASA's Fire Information for Resource Management System (FIRMS (https://firms.modaps.eosdis.nasa.gov/download/). LiDAR records can be found in a public data repository (Huang, 2024). The atmospheric modeling code used is publicly available; instructions for download and operation are given at https://www.camx.com/download/source/.

Acknowledgments
This research is jointly supported by the Ministry of Education, Singapore, under its MOE AcRF Tier 3 Award MOET32022-0006, the Start-up Grant (021452-00001) (LKC) and Start-up Grant (021384-00001) for Assoc. Prof. Yim (ASE), EOS FY2022 funding, the National Research Foundation, Singapore, and National Environment Agency under its Air Quality Monitoring and Control Funding Initiative (AQMC-2023-1D-01). Any opinions, findings and conclusions or recommendations expressed in this material are those of the author(s) and do not reflect the views of National Research Foundation, Singapore and National Environment Agency. The authors would like to acknowledge the High Performance Computing Centre of Nanyang Technological University (NTU) Singapore, for providing the computing resources, facilities, and services that have contributed significantly to this work. In addition, we would like to express our thanks to the technical supports from Centre for Geohazard Observations (CGO) of Earth Observatory of Singapore (EOS) at NTU Singapore, and would also like to acknowledge the support from the Community Engagement Office of EOS at NTU Singapore for creating Figure 4. This work comprises EOS contribution number 575.

References

Algarra, I., Eiras-Barca, J., Nieto, R., & Gimeno, L. (2019). Global climatology of nocturnal low-level jets and associated moisture sources and sinks. *Atmospheric Research*, *229*, 39–59. https://doi.org/10.1016/j.atmosres.2019.06.016

Atwood, S. A., Reid, J. S., Kreidenweis, S. M., Yu, L. E., Salinas, S. V., Chew, B. N., & Balasubramanian, R. (2013). Analysis of source regions for smoke events in Singapore for the 2009 El Nino burning season. *Atmospheric Environment*, *78*, 219–230. https://doi.org/10.1016/j.atmosenv.2013.04.047

Barlow, J. F., Dunbar, T. M., Nemitz, E. G., Wood, C. R., Gallagher, M. W., Davies, F., et al. (2011). Boundary layer dynamics over London, UK, as observed using Doppler lidar during REPARTEE-II. *Atmospheric Chemistry and Physics*, *11*(5), 2111–2125. https://doi.org/10.5194/acp-11-2111-2011

Cheng, F.-Y., Wang, Y.-T., Huang, M.-Q., Lin, P.-L., Lin, C.-H., Lin, P.-H., et al. (2022). Boundary layer characteristics over complex terrain in Central Taiwan: Observations and numerical modeling. *Journal of Geophysical Research: Atmospheres*, *127*(2), e2021JD035726. https://doi.org/10.1029/2021JD035726

Chew, B. N., Campbell, J. R., Salinas, S. V., Chang, C. W., Reid, J. S., Welton, E. J., et al. (2013). Aerosol particle vertical distributions and optical properties over Singapore. *Atmospheric Environment*, *79*, 599–613. https://doi.org/10.1016/j.atmosenv.2013.06.026

Dunker, A. M., Koo, B., & Yarwood, G. (2019). Source apportionment of organic aerosol and ozone and the effects of emission reductions. *Atmospheric Environment*, *198*, 89–101. https://doi.org/10.1016/j.atmosenv.2018.10.042

Emery, C., Liu, Z., Russell, A. G., Odman, M. T., Yarwood, G., & Kumar, N. (2017). Recommendations on statistics and benchmarks to assess photochemical model performance. *Journal of the Air and Waste Management Association*, *67*(5), 582–598. https://doi.org/10.1080/10962247.2016.1265027

Fang, T., Gu, Y., & Yim, S. H. L. (2023). Assessing local and transboundary fine particulate matter pollution and sectoral contributions in Southeast Asia during haze months of 2015–2019. *The Science of the Total Environment*, *912*, 169051. https://doi.org/10.1016/j.scitotenv.2023.169051

Gaydos, T. M., Pinder, R., Koo, B., Fahey, K. M., Yarwood, G., & Pandis, S. N. (2007). Development and application of a three-dimensional aerosol chemical transport model, PMCAMx. *Atmospheric Environment*, *41*(12), 2594–2611. https://doi.org/10.1016/j.atmosenv.2006.11.034

Geiß, A., Wiegner, M., Bonn, B., Schäfer, K., Forkel, R., von Schneidemesser, E., et al. (2017). Mixing layer height as an indicator for urban air quality? *Atmospheric Measurement Techniques*, *10*(8), 2969–2988. https://doi.org/10.5194/amt-10-2969-2017

Granier, C., Darras, S., Denier van der Gon, H., Doubalova, J., Elguindi, N., Galle, B., et al. (2019). The Copernicus Atmosphere Monitoring Service global and regional emissions (April 2019 version). https://doi.org/10.24380/D0BN-KX16

Gu, Y., & Yim, S. H. L. (2016). The air quality and health impacts of domestic trans-boundary pollution in various regions of China. *Environment International*, *97*, 117–124. https://doi.org/10.1016/j.envint.2016.08.004

Guenther, A. B., Jiang, X., Heald, C. L., Sakulyanontvittaya, T., Duhl, T., Emmons, L. K., & Wang, X. (2012). The Model of Emissions of Gases and Aerosols from Nature version 2.1 (MEGAN2.1): An extended and updated framework for modeling biogenic emissions. *Geoscientific Model Development*, *5*(6), 1471–1492. https://doi.org/10.5194/gmd-5-1471-2012

Hansen, A. B., Witham, C. S., Chong, W. M., Kendall, E., Chew, B. N., Gan, C., et al. (2019). Haze in Singapore – Source attribution of biomass burning PM_{10} from Southeast Asia. *Atmospheric Chemistry and Physics*, *19*(8), 5363–5385. https://doi.org/10.5194/acp-19-5363-2019

Hertwig, D., Burgin, L., Gan, C., Hort, M., Jones, A., Shaw, F., et al. (2015). Development and demonstration of a Lagrangian dispersion modeling system for real-time prediction of smoke haze pollution from biomass burning in Southeast Asia. *Journal of Geophysical Research: Atmospheres*, *120*(24), 12605–12630. https://doi.org/10.1002/2015JD023422

Hogan, R. J., Grant, A. L. M., Illingworth, A. J., Pearson, G. N., & O'Connor, E. J. (2009). Vertical velocity variance and skewness in clear and cloud-topped boundary layers as revealed by Doppler lidar. *Quarterly Journal of the Royal Meteorological Society*, *135*(640), 635–643. https://doi.org/10.1002/qj.413

Holben, B. N., Eck, T. F., Slutsker, I., Tanré, D., Buis, J. P., Setzer, A., et al. (1998). AERONET—A federated instrument network and data archive for aerosol characterization. *Remote Sensing of Environment*, *66*(1), 1–16. https://doi.org/10.1016/S0034-4257(98)00031-5

Holloway, T., Fiore, A., & Hastings, M. G. (2003). Intercontinental transport of air pollution: Will emerging science lead to a new hemispheric treaty? *Environmental Science and Technology*, *37*(20), 4535–4542. https://doi.org/10.1021/es034031g

Hou, X., Chan, C. K., Dong, G. H., & Yim, S. H. L. (2019). Impacts of transboundary air pollution and local emissions on PM 2.5 pollution in the Pearl River Delta region of China and the public health, and the policy implications. *Environmental Research Letters*, *14*(3), 034005. https://doi.org/10.1088/1748-9326/aaf493

Huang, H.-Y., Wang, S.-H., Huang, W.-X., Lin, N.-H., Chuang, M.-T., da Silva, A. M., & Peng, C.-M. (2020). Influence of synoptic-dynamic meteorology on the long-range transport of Indochina biomass burning aerosols. *Journal of Geophysical Research: Atmospheres*, *125*(3), e2019JD031260. https://doi.org/10.1029/2019JD031260

Huang, T. (2024). Investigating the interaction between transboundary haze and planetary boundary layer in Singapore [Dataset]. Figshare. https://doi.org/10.6084/m9.figshare.24941790

Huang, T., Li, Y., Cheng, J. C. H., Haywood, J., Hon, K. K., Lam, D. H. Y., et al. (2021). Assessing transboundary-local aerosols interaction over complex terrain using a Doppler LiDAR network. *Geophysical Research Letters*, *48*(12), e2021GL093238. https://doi.org/10.1029/2021GL093238

Huang, T., Yang, Y., O'Connor, E. J., Lolli, S., Haywood, J., Osborne, M., et al. (2021). Influence of a weak typhoon on the vertical distribution of air pollution in Hong Kong: A perspective from a Doppler LiDAR network. *Environmental Pollution*, *276*, 116534. https://doi.org/10.1016/j.envpol.2021.116534

Hyer, E. J., & Chew, B. N. (2010). Aerosol transport model evaluation of an extreme smoke episode in Southeast Asia. *Atmospheric Environment*, *44*(11), 1422–1427. https://doi.org/10.1016/j.atmosenv.2010.01.043

Karamchandani, P., Long, Y., Pirovano, G., Balzarini, A., & Yarwood, G. (2017). Source-sector contributions to European ozone and fine PM in 2010 using AQMEII modeling data. *Atmospheric Chemistry and Physics*, *17*(9), 5643–5664. https://doi.org/10.5194/acp-17-5643-2017

Lee, H.-H., Bar-Or, R. Z., & Wang, C. (2017). Biomass burning aerosols and the low-visibility events in Southeast Asia. *Atmospheric Chemistry and Physics*, *17*(2), 965–980. https://doi.org/10.5194/acp-17-965-2017

Lelieveld, J., Evans, J. S., Fnais, M., Giannadaki, D., & Pozzer, A. (2015). The contribution of outdoor air pollution sources to premature mortality on a global scale. *Nature*, *525*(7569), 367–371. https://doi.org/10.1038/nature15371

Li, Z., Zhu, Y., Wang, S., Xing, J., Zhao, B., Long, S., et al. (2022). Source contribution analysis of PM2. 5 using response surface model and particulate source apportionment technology over the PRD region, China. *The Science of the Total Environment*, *818*, 151757. https://doi.org/10.1016/j.scitotenv.2021.151757

Liu, X.-H., Zhang, Y., Xing, J., Zhang, Q., Wang, K., Streets, D. G., et al. (2010). Understanding of regional air pollution over China using CMAQ, part II. Process analysis and sensitivity of ozone and particulate matter to precursor emissions. *Atmospheric Environment*, *44*(30), 3719–3727. https://doi.org/10.1016/j.atmosenv.2010.03.036

Ma, S., Shao, M., Zhang, Y., Dai, Q., & Xie, M. (2021). Sensitivity of PM2.5 and O3 pollution episodes to meteorological factors over the North China Plain. *The Science of the Total Environment*, *792*, 148474. https://doi.org/10.1016/j.scitotenv.2021.148474

Manninen, A. J., Marke, T., Tuononen, M., & O'Connor, E. J. (2018). Atmospheric boundary layer classification with Doppler lidar. *Journal of Geophysical Research: Atmospheres*, *123*(15), 8172–8189. https://doi.org/10.1029/2017JD028169

Meroni, A., Pirovano, G., Gilardoni, S., Lonati, G., Colombi, C., Gianelle, V., et al. (2017). Investigating the role of chemical and physical processes on organic aerosol modelling with CAMx in the Po Valley during a winter episode. *Atmospheric Environment*, *171*, 126–142. https://doi.org/10.1016/j.atmosenv.2017.10.004

O'Connor, E. J., Hogan, R. J., & Illingworth, A. J. (2005). Retrieving stratocumulus drizzle parameters using Doppler radar and lidar. *Journal of Applied Meteorology*, *44*(1), 14–27. https://doi.org/10.1175/JAM-2181.1

O'Connor, E. J., Illingworth, A. J., Brooks, I. M., Westbrook, C. D., Hogan, R. J., Davies, F., & Brooks, B. J. (2010). A method for estimating the turbulent kinetic energy dissipation rate from a vertically pointing Doppler lidar, and independent evaluation from balloon-borne in situ measurements. *Journal of Atmospheric and Oceanic Technology*, *27*(10), 1652–1664. https://doi.org/10.1175/2010JTECHA1455.1

Pearson, G., Davies, F., & Collier, C. (2009). An analysis of the performance of the UFAM pulsed Doppler lidar for observing the boundary layer. *Journal of Atmospheric and Oceanic Technology*, *26*(2), 240–250. https://doi.org/10.1175/2008JTECHA1128.1

Pentikäinen, P., O'Connor, E. J., Manninen, A. J., & Ortiz-Amezcua, P. (2020). Methodology for deriving the telescope focus function and its uncertainty for a heterodyne pulsed Doppler lidar. *Atmospheric Measurement Techniques*, *13*(5), 2849–2863. https://doi.org/10.5194/amt-13-2849-2020

Reid, J. S., Hyer, E. J., Johnson, R. S., Holben, B. N., Yokelson, R. J., Zhang, J., et al. (2013). Observing and understanding the Southeast Asian aerosol system by remote sensing: An initial review and analysis for the Seven Southeast Asian Studies (7SEAS) program. *Atmospheric Research*, *122*, 403–468. https://doi.org/10.1016/j.atmosres.2012.06.005

Slater, J., Coe, H., McFiggans, G., Tonttila, J., & Romakkaniemi, S. (2021). The effect of black carbon on aerosol-boundary layer feedback: Potential implications for Beijing haze episodes. In *Atmospheric Chemistry and Physics Discussions* (pp. 1–23). https://doi.org/10.5194/acp-2021-139

Slater, J., Coe, H., McFiggans, G., Tonttila, J., & Romakkaniemi, S. (2022). The effect of BC on aerosol–boundary layer feedback: Potential implications for urban pollution episodes. *Atmospheric Chemistry and Physics*, *22*(4), 2937–2953. https://doi.org/10.5194/acp-22-2937-2022

Slater, J., Tonttila, J., McFiggans, G., Connolly, P., Romakkaniemi, S., Kühn, T., & Coe, H. (2020). Using a coupled large-eddy simulation–aerosol radiation model to investigate urban haze: Sensitivity to aerosol loading and meteorological conditions. *Atmospheric Chemistry and Physics*, *20*(20), 11893–11906. https://doi.org/10.5194/acp-20-11893-2020

Sullivan, J. T., Rabenhorst, S. D., Dreessen, J., McGee, T. J., Delgado, R., Twigg, L., & Sumnicht, G. (2017). Lidar observations revealing transport of O3 in the presence of a nocturnal low-level jet: Regional implications for "next-day" pollution. *Atmospheric Environment*, *158*, 160–171. https://doi.org/10.1016/j.atmosenv.2017.03.039

Tang, G., Zhang, J., Zhu, X., Song, T., Münkel, C., Hu, B., et al. (2016). Mixing layer height and its implications for air pollution over Beijing, China. *Atmospheric Chemistry and Physics*, *16*(4), 2459–2475. https://doi.org/10.5194/acp-16-2459-2016

Tong, C. H. M., Yim, S. H. L., Rothenberg, D., Wang, C., Lin, C.-Y., Chen, Y. D., & Lau, N. C. (2018). Assessing the impacts of seasonal and vertical atmospheric conditions on air quality over the Pearl River Delta region. *Atmospheric Environment*, *180*, 69–78. https://doi.org/10.1016/j.atmosenv.2018.02.039

Tonttila, J., O'Connor, E. J., Hellsten, A., Hirsikko, A., O'Dowd, C., Järvinen, H., & Räisänen, P. (2015). Turbulent structure and scaling of the inertial subrange in a stratocumulus-topped boundary layer observed by a Doppler lidar. *Atmospheric Chemistry and Physics*, *15*(10), 5873–5885. https://doi.org/10.5194/acp-15-5873-2015

Tonttila, J., O'Connor, E. J., Niemelä, S., Räisänen, P., & Järvinen, H. (2011). Cloud base vertical velocity statistics: A comparison between an atmospheric mesoscale model and remote sensing observations. *Atmospheric Chemistry and Physics*, *11*(17), 9207–9218. https://doi.org/10.5194/acp-11-9207-2011

Tsiringakis, A., Theeuwes, N. E., Barlow, J. F., & Steeneveld, G.-J. (2022). Interactions between the nocturnal low-level jets and the urban boundary layer: A case study over London. *Boundary-Layer Meteorology*, *183*(2), 249–272. https://doi.org/10.1007/s10546-021-00681-7

Tuononen, M., O'Connor, E. J., Sinclair, V. A., & Vakkari, V. (2017). Low-level jets over Utö, Finland, based on Doppler lidar observations. *Journal of Applied Meteorology and Climatology*, *56*(9), 2577–2594. https://doi.org/10.1175/JAMC-D-16-0411.1

Wei, W., Lv, Z. F., Li, Y., Wang, L. T., Cheng, S., & Liu, H. (2018). A WRF-Chem model study of the impact of VOCs emission of a huge petrochemical industrial zone on the summertime ozone in Beijing, China. *Atmospheric Environment*, *175*, 44–53. https://doi.org/10.1016/j.atmosenv.2017.11.058

Welton, E. J., Campbell, J. R., Spinhirne, J. D., & Iii, V. S. S. (2001). *Global monitoring of clouds and aerosols using a network of micropulse lidar systems*. In *Lidar Remote Sensing for Industry and Environment Monitoring* (Vol. 4153, pp. 151–158). SPIE. https://doi.org/10.1117/12.417040

Wiedinmyer, C., Akagi, S. K., Yokelson, R. J., Emmons, L. K., Al-Saadi, J. A., Orlando, J. J., & Soja, A. J. (2011). The Fire INventory from NCAR (FINN): A high resolution global model to estimate the emissions from open burning. *Geoscientific Model Development*, *4*(3), 625–641. https://doi.org/10.5194/gmd-4-625-2011

Yang, Q., Zhao, T., Tian, Z., Kumar, K. R., Chang, J., Hu, W., et al. (2022). The Cross-Border Transport of PM2.5 from the southeast Asian biomass burning emissions and its impact on air pollution in Yunnan Plateau, Southwest China. *Remote Sensing*, *14*(8), 1886. https://doi.org/10.3390/rs14081886

Yarwood, G., Jung, J., Whitten, G. Z., Heo, G., Mellberg, J., & Estes, M. (2010). Updates to the carbon Bond mechanism for version 6 (CB6). In *9th Annual CMAS Conference, Chapel Hill, NC* (pp. 11–13).

Yim, S. H. L. (2020). Development of a 3D real-time atmospheric monitoring system (3DREAMS) using Doppler LiDARs and applications for long-term analysis and hot-and-polluted episodes. *Remote Sensing*, *12*(6), 1036. https://doi.org/10.3390/rs12061036

Yu, E., Bai, R., Chen, X., & Shao, L. (2022). Impact of physical parameterizations on wind simulation with WRF V3.9.1.1 under stable conditions at planetary boundary layer gray-zone resolution: A case study over the coastal regions of north China. *Geoscientific Model Development*, *15*(21), 8111–8134. https://doi.org/10.5194/gmd-15-8111-2022

Zhu, X., Tang, G., Guo, J., Hu, B., Song, T., Wang, L., et al. (2018). Mixing layer height on the North China Plain and meteorological evidence of serious air pollution in southern Hebei. *Atmospheric Chemistry and Physics*, *18*(7), 4897–4910. https://doi.org/10.5194/acp-18-4897-2018